Received: 10 August 2021 | Accepted: 4 October 2021

DOI: 10.1111/gcb.15938

PRIMARY RESEARCH ARTICLE

Global Change Biology WILEY

Temperature acclimation of leaf respiration differs between marsh and mangrove vegetation in a coastal wetland ecotone

Matthew A. Sturchio[1] | Jeff Chieppa[1,2] | Samantha K. Chapman[3] | Gabriela Canas[1] | Michael J. Aspinwall[1,2]

[1]Department of Biology, University of North Florida, Jacksonville, Florida, USA

[2]School of Forestry and Wildlife Sciences, Auburn University, Auburn, Alabama, USA

[3]Department of Biology and Center for Biodiversity and Ecosystem Stewardship, Villanova University, Villanova, Pennsylvania, USA

Correspondence
Michael J. Aspinwall, School of Forestry and Wildlife Sciences, Auburn University, Auburn, AL 36849, USA.
Email: aspinwall@auburn.edu

Present address
Matthew A. Sturchio, Department of Biology and Graduate Degree Program in Ecology, Colorado State University, Fort Collins, Colorado 80523, USA

Funding information
National Institute of Food and Agriculture, Grant/Award Number: 2019-67013-29161; NSF, Grant/Award Number: 1655659

Abstract

Temperature acclimation of leaf respiration (*R*) is an important determinant of ecosystem responses to temperature and the magnitude of temperature-CO_2 feedbacks as climate warms. Yet, the extent to which temperature acclimation of *R* exhibits a common pattern across different growth conditions, ecosystems, and plant functional types remains unclear. Here, we measured the short-term temperature response of *R* at six time points over a 10-month period in two coastal wetland species (*Avicennia germinans* [C_3 mangrove] and *Spartina alterniflora* [C_4 marsh grass]) growing under ambient and experimentally warmed temperatures at two sites in a marsh–mangrove ecotone. Leaf nitrogen (N) was determined on a subsample of leaves to explore potential coupling of *R* and N. We hypothesized that both species would reduce *R* at 25°C (R^{25}) and the short-term temperature sensitivity of *R* (Q_{10}) as air temperature (T_{air}) increased across seasons, but the decline would be stronger in *Avicennia* than in *Spartina*. For each species, we hypothesized that seasonal temperature acclimation of *R* would be equivalent in plants grown under ambient and warmed temperatures, demonstrating convergent acclimation. Surprisingly, *Avicennia* generally increased R^{25} with increasing growth temperature, although the Q_{10} declined as seasonal temperatures increased and did so consistently across sites and treatments. Weak temperature acclimation resulted in reduced homeostasis of *R* in *Avicennia*. *Spartina* reduced R^{25} and the Q_{10} as seasonal temperatures increased. In *Spartina*, seasonal temperature acclimation was largely consistent across sites and treatments resulting in greater respiratory homeostasis. We conclude that co-occurring coastal wetland species may show contrasting patterns of respiratory temperature acclimation. Nonetheless, leaf N scaled positively with R^{25} in both species, highlighting the importance of leaf N in predicting respiratory capacity across a range of growth temperatures. The patterns of respiratory temperature acclimation shown here may improve the predictions of temperature controls of CO_2 fluxes in coastal wetlands.

KEYWORDS
Avicennia germinans, coastal wetlands, coordination theory, homeostasis, respiratory capacity, *Spartina alterniflora*, thermal acclimation

1 | INTRODUCTION

Roughly, half of terrestrial gross primary production (GPP) is returned to the atmosphere each year via autotrophic respiration (Piao et al., 2013), and approximately half of plant respiration comes from leaves (Atkin et al., 2007, 2015). As a result, leaf respiration (*R*, typically measured in darkness as CO_2 efflux) is an important parameter for simulating carbon (C) cycling in terrestrial biosphere models (TBMs) and associated earth system models (Atkin et al., 2014; Fisher et al., 2014). Leaf *R* is determined by a series of enzymatic reactions in the cytosol and mitochondria and is therefore temperature dependent. In the short term (minutes, hours), *R* increases quasi-exponentially with increasing measurement temperature before reaching an optimum (typically between 50 and 60°C Aspinwall et al., 2017; O'Sullivan et al., 2017). This temperature sensitivity has led to the prediction that climate warming will accelerate the positive feedback between CO_2 and temperature. However, there is considerable evidence that plants may "acclimate" to seasonal or spatial variation in growth temperature by modifying the short-term temperature response of *R*. Many plants acclimate to increasing growth temperatures (increasing seasonal temperatures, experimental warming) by reducing *R* at a set measurement temperature (i.e., 25°C, Slot & Kitajima, 2015). This type of acclimation is referred to as Type II acclimation and is considered a change in respiratory capacity (Atkin & Tjoelker, 2003). Less commonly, plants respond to increasing growth temperatures by reducing the short-term temperature sensitivity of *R* (Q_{10}, activation energy, Slot & Kitajima, 2015). This type of acclimation is referred to as Type I acclimation (Atkin & Tjoelker, 2003). Both Type II and Type I temperature acclimation of *R* result in varying degrees of respiratory homeostasis across a range of prevailing growth temperatures (Slot & Kitajima, 2015). At larger scales, the reduced sensitivity of *R* to temperature (i.e., greater homeostasis) should reduce the positive feedback between temperature and CO_2 as climate warms (King et al., 2006; Smith & Dukes, 2013). Moreover, when TBMs account for temperature acclimation of leaf CO_2 exchange, higher net C storage is predicted under climate warming than would be predicted without temperature acclimation (Lombardozzi et al., 2015; Smith et al., 2016).

Although leaf *R* and patterns and mechanisms of respiratory temperature acclimation are better understood and increasingly represented in TBMs, important knowledge gaps and data uncertainties remain. One uncertainty is whether temperature acclimation of leaf *R* is consistent over time (i.e., seasons), across spatially separated sites, and across plants growing under current and warmed climates. Most evidence for temperature acclimation of leaf *R* comes from three types of studies: field studies of plants responding to seasonal variation in temperature at individual sites (Atkin et al., 2000; Lee et al., 2005; Ow et al., 2008, 2010; Tjoelker et al., 2008, 2009), field studies that implement warming overtop natural seasonal temperature changes (Aspinwall et al., 2016; Bruhn et al., 2007), and warming studies conducted under controlled conditions on small plants, usually for short time periods (Bolstad et al., 2003; Cheesman & Winter, 2013; Drake et al., 2015). Acclimation responses observed across all studies could be the result of a common mechanism. Indeed, two experiments with tree species from warm-temperate and boreal climates showed that seasonal temperature acclimation of *R* was equivalent between trees grown under ambient and experimentally warmed temperatures, indicating convergent acclimation (Aspinwall et al., 2016; Reich et al., 2016). Thus, physiological responses to climate warming might be predicted from studies of physiological responses to seasonal temperature changes. There is also evidence that temperature acclimation over time and temperature acclimation across space may result in similar changes in leaf *R* (Vanderwel et al., 2015). However, additional experiments are required to determine whether plants show convergent patterns of temperature acclimation of leaf *R* over seasons, sites, and with climate warming. This will help determine whether temperature acclimation responses are common and generalizable across a wide range of environmental conditions.

Whether temperature acclimation of leaf physiology differs between C_3 and C_4 plants is also an important uncertainty. It has been hypothesized that C_4 plants may show limited capacity for temperature acclimation due to a more complex physiology (Yamori et al., 2014). Support for this hypothesis is mixed. Yamori et al. (2014) synthesized results from individual studies with different methodologies and growth temperatures and found that C_3 plants generally showed greater ability for photosynthetic temperature acclimation than C_4 plants. However, Smith and Dukes (2017) grew several C_3 and C_4 species together in a controlled environment under similar temperature treatments and found that C_3 and C_4 plants showed comparable temperature acclimation of photosynthesis and leaf *R* (Smith & Dukes, 2017). Additional studies that compare temperature acclimation of C_3 and C_4 species will help clarify whether predictions of temperature acclimation responses need to be photosynthetic-type specific.

Leaf *R* and temperature acclimation of leaf *R* also remain understudied in some regions and ecosystems, including coastal wetlands. These ecosystems are typically dominated by C_4 marsh grass species and C_3 mangrove species. Despite covering a small proportion of the earth's surface, coastal marsh and mangrove ecosystems play an important role in global C cycling (Bouillon et al., 2008; Donato et al., 2011; Lu et al., 2017; Lugo & Snedaker, 1974; Mcleod et al., 2011). These ecosystems have high rates of C accumulation and burial, slow decomposition rates, and a relatively high fraction of biomass belowground. Autotrophic *R* (a large proportion of which is leaf *R*) is a major component of the coastal wetland C cycle, accounting for an estimated ~50% of GPP in marsh and mangrove ecosystems (Alongi, 2020). However, direct measures of leaf *R* or its temperature sensitivity over space and time are relatively rare for marsh and mangrove species. Only a handful of studies have quantified temperature acclimation of leaf *R* in mangrove species (see Akaji et al., 2019; Aspinwall et al., 2021) and none have examined temperature acclimation in marsh grasses. As a result, the extent to which temperature acclimation of *R* leads toward homeostasis of realized (in situ) *R* over space and time in coastal wetland plants remains unclear.

Studies that examine the patterns of temperature acclimation of leaf *R* over space and time may provide insight into spatial and temporal variability in photosynthetic capacity. Respiration plays an important role in several processes that influence photosynthesis including nitrate reduction, phloem loading and turnover of phospholipid membranes and proteins. Rubisco accounts for a large fraction of leaf protein in C_3 plants (Aspinwall et al., 2019; Evans, 1989; Hikosaka & Shigeno, 2009) and respiratory-driven turnover of Rubisco is important for maintaining photosynthetic capacity under natural conditions. This likely explains why leaf *R* and maximum rates of Rubisco carboxylation (V_{cmax}) (both measured at 25°C) are positively related across a wide range of C_3 species (Atkin et al., 2015; O'Leary et al., 2019; Wright et al., 2004). Recent analyses also support the theory that temperature acclimation of leaf *R* helps maintain "optimal" photosynthetic capacity in C_3 species (Wang et al., 2020). Leaf *R* data are limited for C_4 species (Atkin et al., 2015) such that broadscale photosynthesis–respiration relationships are unclear across C_4 species, although similar coupling of *R* and photosynthesis is expected.

The coupling of photosynthetic and respiratory capacity may be related to total leaf N, which represents total photosynthetic and respiratory enzyme content. Indeed, across C_3 species, leaf N scales positively with both V_{cmax} and *R* at 25°C (Atkin et al., 2015; Reich et al., 2008; Walker et al., 2014). In C_4 species, positive relationships between leaf N and net photosynthesis have also been observed (Ghannoum et al., 2005), although leaf N–leaf *R* relationships have not been widely explored. Similar coupling of leaf N, V_{cmax}, and *R* across changing growth temperatures is sometimes observed within C_3 species growing at individual sites (Crous et al., 2017; Lee et al., 2005; Tjoelker et al., 1999). Thus, changes in leaf N may also partly explain coordinated temperature acclimation of leaf *R* and photosynthetic capacity (Wang et al., 2020). For these reasons, many land surface models predict functional-type specific rates of *R* using either leaf N on an area or mass basis or estimates of V_{cmax} at 25°C (Fisher et al., 2014; Lawrence et al., 2019).

In this study, we repeatedly measured the short-term temperature responses of leaf *R* over a 10-month period in a C_3 mangrove species (*Avicennia germinans*) and C_4 marsh grass species (*Spartina alterniflora*) grown in situ under ambient temperatures and experimental warming at two spatially separated sites in a marsh–mangrove ecotone on the Atlantic coast of Florida (USA). The ecotone represents a transitional zone where the southern part of temperate salt marsh habitat converges with the northern limit of tropical mangrove habitat. From each short-term temperature response measurement, we estimated *R* at 25°C (R^{25}) and the short-term temperature sensitivity of leaf *R* (Q_{10}). We also used individual short-term temperature response measurements to estimate realized (in situ) *R* at prevailing air temperatures. We determined leaf N on a subset of leaves collected at both sites, in both treatments, on different measurement dates. For each species, we hypothesized that R^{25} and the short-term Q_{10} of *R* would decrease with experimental warming and as seasonal air temperatures increased. Importantly, we expected that the decline in R^{25} and the short-term Q_{10} of *R* with increasing seasonal temperatures would be equivalent in plants growing under ambient and warmed temperatures at both sites, demonstrating convergent temperature acclimation of *R*. However, given that C_4 species may show lower capacity for temperature acclimation than C_3 species (Yamori et al., 2014), we hypothesized that acclimation responses would be greater in *Avicennia* than in *Spartina*. In turn, we expected greater homeostasis of realized *R* across a range of prevailing growth temperatures in *Avicennia* than in *Spartina*. Finally, for each species, we hypothesized that leaf N concentrations would scale positively with R^{25} over time and across sites and treatments, providing an explanation for convergent temperature acclimation of *R*.

2 | MATERIALS AND METHODS

2.1 | Study sites and experimental design

This study took place at two sites in the Guana Tolomato Matanzas National Estuarine Research Reserve (GTMNERR) on the Atlantic coast of Florida, near St. Augustine. The estuarine vegetation in GTMNERR represents a marsh–mangrove ecotone. The southern part of salt marsh habitat converges and overlaps with the northern limit of mangrove habitat in Florida, although mangroves are increasingly common north of GTMNERR (Dix et al., 2021). The north site (NS) was located roughly 14 km north of St. Augustine along the Tolomato River near the northern edge of GTMNERR (30°00'41.9"N, 81°20'39.2"W). The south site (SS) was located roughly 20 km south of St. Augustine (34 km to the south of NS) and just north of the Matanzas Inlet (29°43'38.3"N, 81°14'25.0"W). NS and SS have similar elevations, and average annual precipitation at the GTMNERR reserve is 1317 mm (Chapman et al., 2021). Mean annual temperature (2001–2018) at St. Augustine is 20.8°C. The highest monthly mean daily max temperature (July) is 32.0°C, and the lowest monthly mean daily low temperature (January) is 11.1°C (NOAA-NCDC). *Spartina alterniflora* (smooth cordgrass) and *A. germinans* (black mangrove) are common at both sites although *Avicennia* trees are generally larger and more abundant at SS. *Spartina* is a C_4 grass (PEP-CK subtype) that dominates temperate estuaries along the east coast of North America and warm-temperate estuaries in the Gulf of Mexico and northern Florida (Lugo et al., 1999). *Avicennia* is a broadly distributed mangrove species native to warm-temperate, subtropical, and tropical regions of the Americas and Africa. On the Atlantic coast, its distribution stretches from North Florida to southern Brazil. All mangroves selected for this study ranged from 4 to 11 years old in 2018 with an average age of 7.4 and 7.2 years at SS and NS, respectively (Chapman et al., 2021).

The study included six replicates of four treatment plots at each site. The four treatments were: *Avicennia* ambient, *Avicennia* warmed, *Spartina* ambient, and *Spartina* warmed (Chapman et al., 2021). Treatment plots were randomly positioned within a 1-ha area at each site. The warmed plots were enclosed in 1.5 m × 1.5 m × 1.5 m chambers, framed with PVC and wrapped in 6 mil polyethylene greenhouse film (Greenhouse Megastore) that transmits ~90% of photosynthetically active radiation. The chamber top was left open to allow for air circulation (mixing) and natural rainfall. The chambers "trap" radiation causing the chamber air to passively warm. Consequently, only daytime warming is achieved using this design with minimal warming occurring during cloudy weather, when radiation is limited, or at night. However, unlike infrared heaters, chambers warm air temperatures rather than canopy surface temperatures (e.g., De Boeck et al., 2012; Smith et al., 2020) and do not inhibit dew formation (Feng et al., 2021). In the event of a tropical storm, we removed the polyethylene film from the PVC frames so that chambers would not become airborne. At each site, air temperature (T_{air}) and relative humidity (RH) were measured every 30 min in the center of two ambient and warmed treatment plots per species using an air temperature/RH sensor covered in a solar radiation shield (HOBO MX2302 External Temperature/RH Sensor; Onset Computer Corp.).

Daily maximum, mean, and minimum T_{air}, RH, and vapor pressure deficit at both sites and treatments (averaged across species) are shown in Figure S1. Averaged over time, mean daily T_{air} was 0.63 and 0.66°C higher in warmed plots than in the ambient plots at NS and SS (Figure S2a,c), respectively (NS ambient mean daily T_{air} = 22.8 ± 5.1 [standard deviation] °C, NS warmed mean daily T_{air} = 23.5 ± 5.3; SS ambient mean daily T_{air} = 22.9 ± 5.1°C, SS warmed mean daily T_{air} = 23.6 ± 5.4°C). Daily maximum T_{air} was on average 3.1 and 3.2°C higher in the warmed plots than in the ambient plots at NS and SS (Figure S2b,d), respectively (NS ambient daily max T_{air} = 28.1 ± 5.2°C, NS warmed mean daily T_{air} = 31.2 ± 5.8°C; SS ambient daily max T_{air} = 27.5 ± 5.2°C, SS warmed daily max T_{air} = 30.7 ± 5.8°C). Warming of this magnitude (1–3°C) is expected by 2050 throughout the southeast United States (Ashfaq et al., 2016). Daily mean RH was similar between treatments and sites and averaged 83.1 ± 7.1% and 85.3 ± 8.4% at NS and SS, respectively (Figure S1b,e). Daily mean VPD was generally <1 at both sites, with only small differences in VPD between warmed and ambient treatment plots (Figure S1c,f).

2.2 | Temperature response of leaf respiration

Measurements of the short-term temperature response of leaf dark respiration (*R*) were conducted at six time points (October, December, February, April, June, and July) over a 10-month period. Each measurement campaign was split over a maximum of 2 days at each site (4 days total). On each measurement day, we collected two entire recent and fully developed upper canopy leaves from each *Spartina* plot and three recent and fully developed upper canopy leaves from each *Avicennia* plot. *Spartina* leaves were excised ~2 cm distal to the ligule. Leaves were collected predawn (04:30–06:00 local time) to avoid the activation of photosynthesis. The excised leaves were placed in Ziplock bags with moist paper and transferred to the laboratory in complete darkness. Previous studies have found no effect of leaf removal on *R* measurements (Aspinwall et al., 2017, 2019; O'Sullivan et al., 2013). All measurements were completed the same day as leaf collection. We found no evidence that *R* changed with time since leaf removal; rates of *R* at 20°C did not vary with time of day in either species. Leaf area (cm^2) of the measured leaves was determined with a leaf area meter (LI-3000C; LI-COR BioSciences) just prior to measurements of *R*. Leaf area data were used to calculate *R* per unit area (R_{area} μmol m^{-2} s^{-1}).

Short-term temperature response curves of *R* were completed by sealing all excised leaves inside a large gas-exchange chamber (3010-GWK1; Heinz Walz GmbH) connected to a portable infrared gas analyzer (LI-6400XT; LiCor Inc.). The large gas-exchange chamber was set at 20°C, while the flow rate and reference CO_2 (controlled by the infrared gas-analyzer) were set at 500 mol s^{-1} and 410 μmol mol^{-1}, respectively. T_{leaf} on the abaxial surface of the leaf was continuously measured with a small-gauge copper constantan thermocouple wire attached to a LI-6400XT external thermocouple adaptor (LI6400-13). To facilitate measurements of *R*, the airflow from the chamber was connected to the "sample" gas line of the LI-6400XT fitted with an empty and closed 2 × 3 cm cuvette. The incoming air was dried before entering the 3010-GWK1 chamber by routing the incoming air through the LI-6400XT desiccant column. Once rates of *R* reached steady state at 20°C (~5 min), the chamber temperature was increased from 20 to 40°C at a rate of 1°C per minute using the chamber software (GFS-Win; Heinz Walz GmbH) while continuously (30 s interval) measuring R_{area} and T_{leaf}. Each short-term temperature response measurement took approximately 25 min to complete. After temperature response measurements were completed, leaves were dried at 70°C for ~72 h after which leaf dry mass was determined and leaf dry mass per unit area (LMA, g m^{-2}) was calculated. Leaf *R* per unit mass (R_{mass}, nmol g^{-1} s^{-1}) was calculated by dividing R_{area} (×1000) by LMA. All individual short-term temperature response curves of R_{area} and R_{mass} are shown in Figures S3 and S4. Each individual measurement leaf was ground into a fine powder with a ball mill and dried at 105°C for ~16 h, stored under desiccation, and leaf N per unit mass (N_{mass}, % or g N kg^{-1}) was determined using a combustion elemental analyzer (Rapid MAX N; Elementar Americas Inc.). Leaf N per unit area (N_{area}, g N m^{-2}) was calculated as the product of %N and LMA.

2.3 | Modeling the temperature response of respiration

Nonlinear regression was used to model the temperature response of leaf *R* (area and mass basis). Nonlinear models were fit using Rstudio (R v.3.6.1, Rstudio v.1.2.1335; R Core Team, 2013). We compared the suitability of three algorithms: (1) a polynomial function, which describes the nonlinear relationship between ln-transformed *R* and T_{leaf} (Heskel et al., 2016; Patterson et al., 2018), (2) an exponential function with a single Q_{10} value (Ryan, 1991), and (3) a modified Arrhenius function (Lloyd & Taylor, 1994). The polynomial function is written as:

$$\ln R = a + bT + cT^2 \quad (1)$$

or

$$R = e^{a + bT + cT^2}, \quad (2)$$

where T is T_{leaf} and a is an estimate of ln R at 0°C, b is the slope of temperature response of ln R at 0°C, and c describes any nonlinearity in the temperature response of ln R with increasing T_{leaf}. The differential of Equation 2 can be used to estimate the Q_{10} of R at any T_{leaf}:

$$Q_{10} = e^{10 \times (b + 2cT)}. \quad (3)$$

The polynomial function (Equation 1) provided the best fit to our data (all $R^2 > 0.98$, all $p < .0001$), with a strong linear relationship between observed and predicted values of ln R ($R^2 = .998$), and residual values normally distributed around zero with little pattern associated with increasing T_{leaf}. Thus, we used the polynomial equation to model the temperature response of R and used coefficients a, b and c to estimate R_{area} and R_{mass} at 25°C (R^{25}_{area}, R^{25}_{mass}), and the Q_{10} of R at 25°C (Q^{10}_{25}) for each leaf. Mean (± standard error) values of a, b, and c for each species, time point, site, and treatment are provided in Tables S1 and S2.

To determine how seasonal changes in the short-term temperature response of R (i.e., seasonal temperature acclimation) influenced realized rates of R in both species, we used parameters a, b, and c (Equations 1 and 2) from individual temperature response curves to estimate realized (in situ) R (area and mass basis) at the prevailing mean daily T_{air} when sampling took place. We separated the data by species, site, and treatment and determined the long-term temperature sensitivity of realized R using an exponential function (Ryan, 1991) that estimates the Q_{10} of R (constant across the measurement temperature range) and R at a reference temperature of 18°C (R_{18}) which is near the lowest mean daily T_{air} across sites and treatments. For each species, we compared Q_{10} and R_{18} estimates between sites and treatments by calculating 95% confidence intervals (standard error × 1.96). When confidence intervals for Q_{10} and R_{18} did not overlap between sites or treatments, we fit separate temperature response functions for each site or treatment. If confidence intervals overlapped, suggesting that parameters were not different between sites or treatments, we fit a single temperature response function across all data.

We also quantified the degree of respiratory homeostasis *across seasons* by calculating a temperature acclimation ratio for each measurement date following Slot and Kitajima (2015): Acclim_{homeo} = R at lowest mean daily T_{air}/R at mean daily T_{air}. The numerator is individual estimates of in situ R at the coolest time point (i.e., lowest mean daily T_{air}; held constant), and the denominator is individual estimates of in situ R, for the same treatment plot, estimated at each time point warmer than the coolest time point. Ratios were calculated separately for each species, site, and treatment. Ratios >1 indicate temperature acclimation resulting in "overcompensation," ratios = 1 indicate temperature acclimation resulting in complete homeostasis, and ratios <1 indicate temperature acclimation resulting in partial homeostasis (Slot & Kitajima, 2015). Ratios were plotted against the change in prevailing mean daily T_{air} across seasons to assess changes respiratory homeostasis with increasing seasonal temperatures.

2.4 | Data analysis

All analyses were performed using Rstudio (R v.3.6.1, Rstudio v.1.2.1335; R Core Team, 2013). As a preliminary step, we carried out variance partitioning to determine the proportion of the overall variance in each trait (e.g., R^{25}_{area}) explained by different experimental factors (species, measurement dates, site, treatment). The variance partitioning results indicated that "species" accounted for most of the trait variance (16%–68%), while other factors generally explained a much smaller proportion of the variance (0%–7%) (Figure S5). Therefore, the remainder of the analysis was conducted separately for each species.

For each species, we used analysis of variance (ANOVA) to test the effects of measurement date (i.e., time), temperature treatment (ambient, warmed), site (NS, SS), and their respective interactions on R^{25}_{area}, R^{25}_{mass}, Q^{10}_{25}, LMA, N_{mass}, and N_{area}. For consistency, we analyzed predicted values of R^{25}_{area} and R^{25}_{mass} derived from our temperature response models rather than observed values at 25°C, although predicted and observed values were nearly identical given the high resolution of our temperature response data. Homogeneity of variance for model results were tested using Levene's and Shapiro–Wilk tests. Data were log or square-root transformed as necessary.

For each species, analysis of covariance (ANCOVA) was used to test relationships between R^{25}_{area}, R^{25}_{mass}, Q^{10}_{25}, LMA, N_{mass}, and N_{area} values and mean daily T_{air} of the preceding 7 days and determine whether relationships differed between sites or treatments. If seasonal temperature acclimation of leaf R occurred, we expected negative linear relationships between mean daily T_{air} and R^{25}_{area}, R^{25}_{mass}, or Q^{10}_{25}. The strength of acclimation is indicated by the slope of this relationship; a more negative slope estimate indicates stronger acclimation. In this model, site and treatment were treated as factors and mean daily T_{air} a covariate. A significant ($p < .05$) interaction between mean daily T_{air} and site or treatment indicated that site or treatment affected the relationship between mean daily T_{air} and the response variable (e.g., R^{25}_{area}), and different slope parameters were required for each site or treatment. If site, treatment, and mean daily T_{air} were significant ($p < .10$), with no interactions, equations with different intercepts for each site or treatment, but a common slope, were fit to the data. If only mean daily T_{air} was significant, one equation describing the relationship between mean daily T_{air} and the response variable was fit to data from both sites and treatments. ANCOVA was also used to test whether leaf N (N_{mass}, N_{area}) scales positively with respiratory capacity (R^{25}_{area},R^{25}_{mass}), and whether site or treatment changes the relationship between leaf N and respiratory capacity. In addition, ANCOVA was used to test relationships between Acclim_{homeo} (measure of respiratory homeostasis) and the change in mean daily T_{air} over time, and potential modifying effects of site or treatment.

3 | RESULTS

3.1 | Leaf R, leaf N, and LMA over time, sites, and temperature treatments

In *Avicennia*, R^{25}_{area}, R^{25}_{mass}, and N_{area} varied over time, but temporal differences in these traits depended upon site (significant date × site interactions, Table 1). R^{25}_{area} was higher at NS than at SS in December 2019 (NS: 1.09 ± 0.04 μmol m^{-2} s^{-1} and SS: 0.86 ± 0.04 μmol m^{-2} s^{-1}), but lower at NS than at SS in July 2020 (NS: 1.05 ± 0.04 μmol m^{-2} s^{-1} and SS: 1.30 ± 0.04 μmol m^{-2} s^{-1}, Figure 1a). R^{25}_{mass} was also lower at NS than at SS in July 2020 (NS: 4.36 ± 0.36 nmol g^{-1} s^{-1} and SS: 7.64 ± 0.36 nmol g^{-1} s^{-1}, Figure 1c). N_{area} was higher at NS (4.29 ± 0.17 g N m^{-2}) than at SS (3.22 ± 0.23 g N m^{-2}) in October 2019 (Figure 1i). R^{25}_{area}, R^{25}_{mass}, and N_{area} were similar between sites at the remaining time points.

Across both sites, warming increased *Avicennia*R^{25}_{area} by 8% (ambient R^{25}_{area} = 1.05 ± 0.02 μmol m^{-2} s^{-1} and warmed R^{25}_{area} = 1.14 ± 0.02 μmol m^{-2} s^{-1}). However, warming effects on R^{25}_{mass} differed between sites (treatment × site interaction, Table 1). Warming did not affect R^{25}_{mass} at NS (mean = 4.43 ± 0.21 nmol g^{-1} s^{-1}) but increased R^{25}_{mass} by 24% at SS (ambient R^{25}_{mass} = 4.56 ± 0.22 nmol g^{-1} s^{-1} and warmed R^{25}_{mass} = 5.67 ± 0.23 nmol g^{-1} s^{-1}).

In *Avicennia*, Q^{10}_{25} varied over time (Table 1) and was highest in February and April 2020 (2.25 ± 0.05 and 2.26 ± 0.05, respectively), and lowest in June 2020 (1.94 ± 0.05, Figure 1e). Q^{10}_{25} did not differ between treatments but differed between sites (Table 1). Q^{10}_{25} was lower at NS (2.03 ± 0.03) than at SS (2.17 ± 0.03). LMA showed a complex pattern; with variation over time depending upon both treatment and site (treatment × date × site, Table 1) (Figure 2g). LMA was highest in warmed plants at NS in July 2020 (272 ± 10.4 g m^{-2}) and October 2019 (277 ± 10.4 g m^{-2}), and lowest in ambient plants at SS in July 2020 (168 ± 10.4 g m^{-2}). N_{mass} did not differ between sites or treatments (Table 1), but was 15% higher in June 2020 (17.1 ± 0.60 g N kg^{-1}) than in February 2020 (14.9 ± 0.60 g N kg^{-1}).

In *Spartina*, R^{25}_{area}, R^{25}_{mass}, and LMA varied over time, but temporal variation in these traits depended upon site (i.e., date × site interaction, Table 1; Figure 2). Although date × site interactions were significant for R^{25}_{area}, post hoc analysis revealed that differences between sites occurred on different dates (October 2019, R^{25}_{area} was higher at SS [1.71 ± 0.11 μmol m^{-2} s^{-1}] than at NS in February 2020 [1.19 ± 0.10 μmol m^{-2} s^{-1}] [Figure 1b]). R^{25}_{mass} was generally higher during winter (December, February) and lower during summer (June, July) (Figure 1). In December 2019, R^{25}_{mass} was significantly higher at NS (13.6 ± 0.5 nmol g^{-1} s^{-1}) than at SS (9.9 ± 0.5 nmol g^{-1} s^{-1}). R^{25}_{mass} was similar between sites across all other dates. LMA showed the opposite seasonal pattern of R^{25}_{mass}; lowest in winter and highest during peak growing season. In February 2020, LMA was significantly lower at NS (99 ± 5.9 g m^{-2}) than at SS (128 ± 5.9 g m^{-2}). On average, warming reduced R^{25}_{mass} 6.4% across all time points (Table 1, ambient R^{25}_{mass}: 10.9 ± 0.2 nmol g^{-1} s^{-1} and warmed R^{25}_{mass}: 10.2 ± 0.2 nmol g^{-1} s^{-1}) but had no effect on R^{25}_{area} or LMA.

In *Spartina*, Q^{10}_{25} was similar across sites and treatments (Table 1) but varied over time and was higher in February 2020 (1.94 ± 0.03) than in June 2020 (1.77 ± 0.03) (Figure 1e). Temporal variation in N_{mass} depended upon temperature treatment (significant date × treatment interaction, Table 2). In February 2020, N_{mass} was significantly lower in warmed plants (15.7 ± 0.6 g N kg^{-1}) than in ambient plants (18.3 ± 0.6 g N kg^{-1}) (Figure 1k). N_{area} did not differ between dates, treatments, or sites (and no interactions, Table 1) and averaged (2.04 ± 0.08 g N m^{-2}).

3.2 | Growth temperature–leaf trait relationships

For *Avicennia*, ANCOVA results indicated that the response of R^{25}_{area} and R^{25}_{mass} to mean daily T_{air} differed between sites (T_{air} × site interaction, Table 2). At NS, R^{25}_{area} and R^{25}_{mass} showed no clear relationship with mean daily T_{air} (Figure 2a,c). At SS, R^{25}_{area} and R^{25}_{mass} both increased with increasing mean daily T_{air} (Figure 2a,c; Table S3). In agreement with our ANOVA results, we found that warming generally increased R^{25}_{area} and R^{25}_{mass} in *Avicennia* (Figure 2a,c). These results provide no evidence for temperature acclimation of respiratory capacity (Type II acclimation) in *Avicennia* growing at the species northern range limit. However, Q^{10}_{25} decreased as mean daily T_{air} increased (Table 2; Figure 2e), indicating Type I temperature acclimation. This acclimation response was consistent across treatments and sites, although the intercept of the relationship was lower at NS than at SS (Table 2; Figure 2e; Table S3).

In *Avicennia*, LMA decreased as mean daily T_{air} increased, but the slope of the relationship differed between sites (T_{air} × site interaction, Table 2; Table S3). LMA decreased faster with increasing T_{air} at SS than at NS (Figure 2g; Table S3). Similar to our ANOVA results, warming effects on LMA differed between sites (treatment × site interaction, Table 2). Warming did not change LMA at NS but reduced LMA at SS. Lastly, N_{mass} increased as mean T_{air} increased and did so consistently across treatments and sites (Table 2; Figure 2i).

Spartina showed clear evidence of Type II and Type I temperature acclimation of *R* across seasons, which was consistent across treatments and sites. Specifically, R^{25}_{mass} decreased with increasing mean daily T_{air}; the intercept of the relationship was higher at NS than at SS (Table 2; Figure 2d; Table S3). This relationship accounts for increasing LMA with T_{air} (Figure 2h). Q^{10}_{25} also decreased with increasing mean daily T_{air} and did so consistently across sites and treatments (Figure 2f; Table S3). N_{mass} declined with increasing T_{air}, although the decline in N_{mass} with increasing T_{air} differed between treatments (T_{air} × treatment interaction, Table 2; Figure 2j). Across sites, warming reduced the intercept and slope of the relationship between T_{air} and N_{mass} (Figure 2j; Table S3). N_{area} showed no relationship with mean daily T_{air} in either species.

TABLE 1 Results of a three-way analysis of variance testing the main and interactive effects of temperature treatment (*T*), measurement date (*D*), and site (*S*) on rates of leaf dark respiration per unit area and per unit mass at 25°C ($R^{25}_{area}, R^{25}_{area}, R^{25}_{mass}$), the temperature sensitivity of *R* estimated at 25°C (Q^{10}_{25}), leaf dry mass per unit area (LMA), and leaf nitrogen on per unit area and per unit mass (N_{mass}, N_{area}) in *Spartina alterniflora* and *Avicennia germinans*. Degrees of freedom (*df*) and *F*-values are presented for each factor and response variable. *F*-values with "*," "**," and "***" are significant at $p < .05$, $p < .01$, and $p < .001$, respectively

		Treatment (*T*)		Date (*D*)		Site (*S*)		$T \times D$		$T \times S$		$D \times S$		$T \times D \times S$	
Species	**Trait**	df	*F*	df	*F*	df	*F*	df	*F*	df	*F*	df	*F*	df	*F*
Avicennia germinans	R^{25}_{area}	1	9.05**	5	10.00***	1	0.50	5	0.35	1	1.92	5	5.96***	5	0.48
	R^{25}_{mass}	1	6.79*	5	10.09***	1	9.38**	5	0.34	1	5.27*	5	7.57***	5	0.86
	Q^{10}_{25}	1	0.39	5	9.88***	1	19.38***	5	0.63	1	0.57	5	1.39	5	0.32
	LMA	1	1.95	5	13.29***	1	32.77***	5	0.83	1	6.18*	5	3.87**	5	2.41*
	N_{mass}	1	0.83	2	3.34*	1	0.44	2	0.14	1	0.20	2	0.57	2	0.42
	N_{area}	1	0.05	2	0.08	1	9.18**	2	1.34	1	3.46	2	3.69*	2	0.09
Spartina alterniflora	R^{25}_{area}	1	1.75	5	3.17*	1	0.69	5	0.58	1	0.42	5	2.33*	5	0.49
	R^{25}_{mass}	1	4.83*	5	15.67***	1	12.03***	5	0.51	1	2.68	5	3.53**	5	0.22
	Q^{10}_{25}	1	2.76	5	4.62***	1	0.62	5	0.73	1	2.43	5	0.82	5	0.66
	LMA	1	0.04	5	22.57***	1	2.88	5	0.54	1	0.42	5	4.29**	5	0.37
	N_{mass}	1	0.41	2	15.32***	1	1.82	2	5.55**	1	0.01	2	0.86	2	0.43
	N_{area}	1	0.02	2	2.03	1	1.23	2	2.20	1	0.42	2	1.68	2	0.21

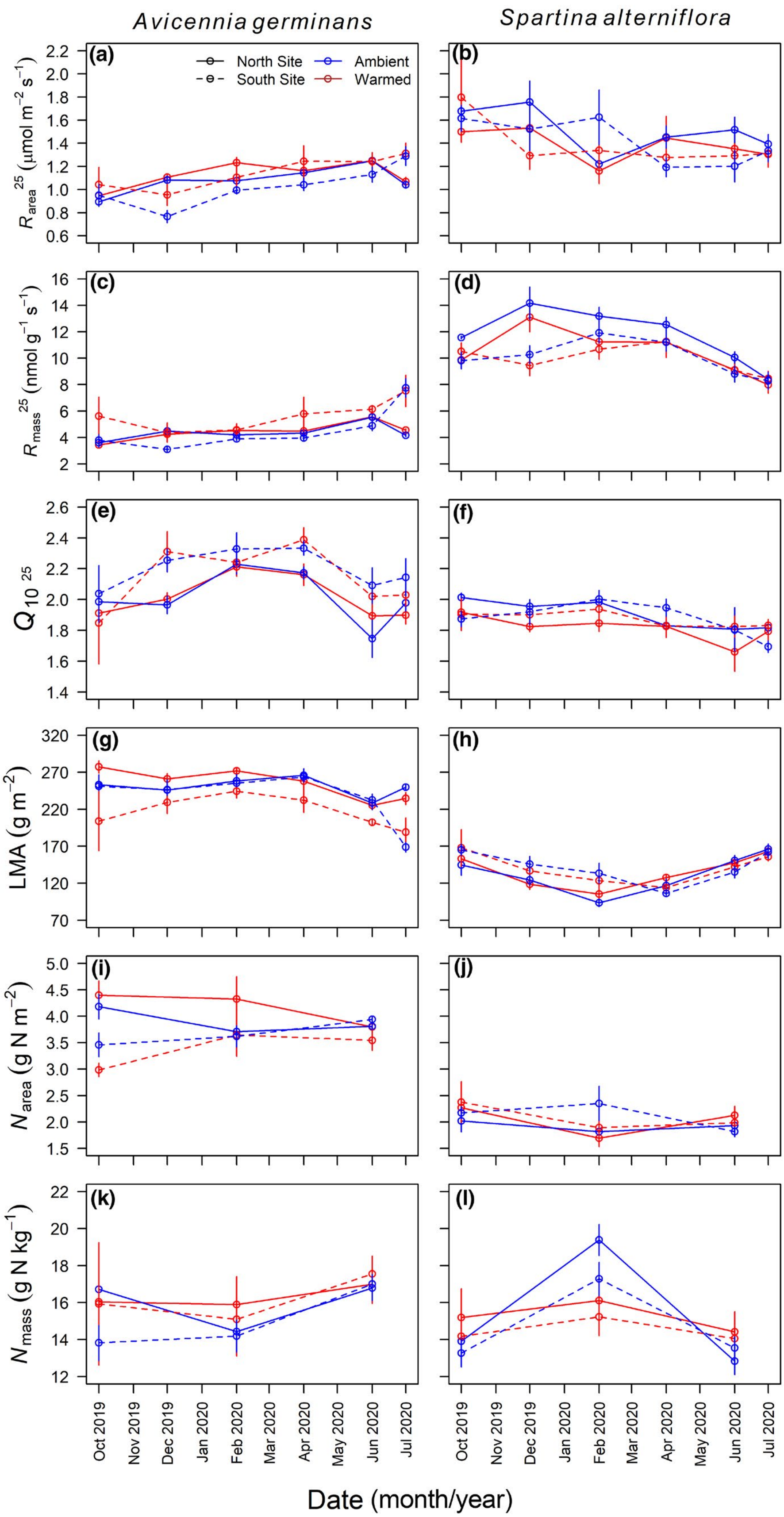

FIGURE 1 Mean values (±standard error, $n = 6$) for several leaf traits over time in *Avicennia germinans* and *Spartina alterniflora* growing at two sites in North Florida (North, South) under two temperature treatments (ambient and warmed). Variable descriptions: R_{area}^{25}, leaf respiration per unit area at 25°C (panels a, b); R_{mass}^{25}, leaf respiration per unit mass at 25°C (panels c, d); Q_{25}^{10}, the temperature sensitivity of R estimated at 25°C (panels e, f); LMA, leaf mass per unit area (panels g, h); N_{area}, leaf N per unit area (panels i, j); N_{mass}, leaf N per unit mass (panels k, l)

FIGURE 2 The relationship between thermal history (mean daily air temperature (T_{air}) of preceding 7 days) and leaf physiological traits for *Avicennia germinans* and *Spartina alterniflora* growing at two sites in North Florida (North, South) under two temperature treatments (ambient and warmed). Variable descriptions: R^{25}_{area}, leaf respiration per unit area at 25°C (panels a, b); R^{25}_{mass}, leaf respiration per unit mass at 25°C (panels c, d); Q^{10}_{25}, the temperature sensitivity of *R* estimated at 25°C (panels e, f); LMA, leaf mass per unit area (panels g, h); N_{area}, leaf N per unit area (panels i, j); N_{mass}, leaf N per unit mass (panels k, l). Gray solid lines signify a common relationship across sites and treatments. Black solid and dashed lines signify different relationships between sites. Red and blue lines signify different relationships between treatments that are consistent across sites. Intercept and slope parameters for the relationships are provided in Table S3)

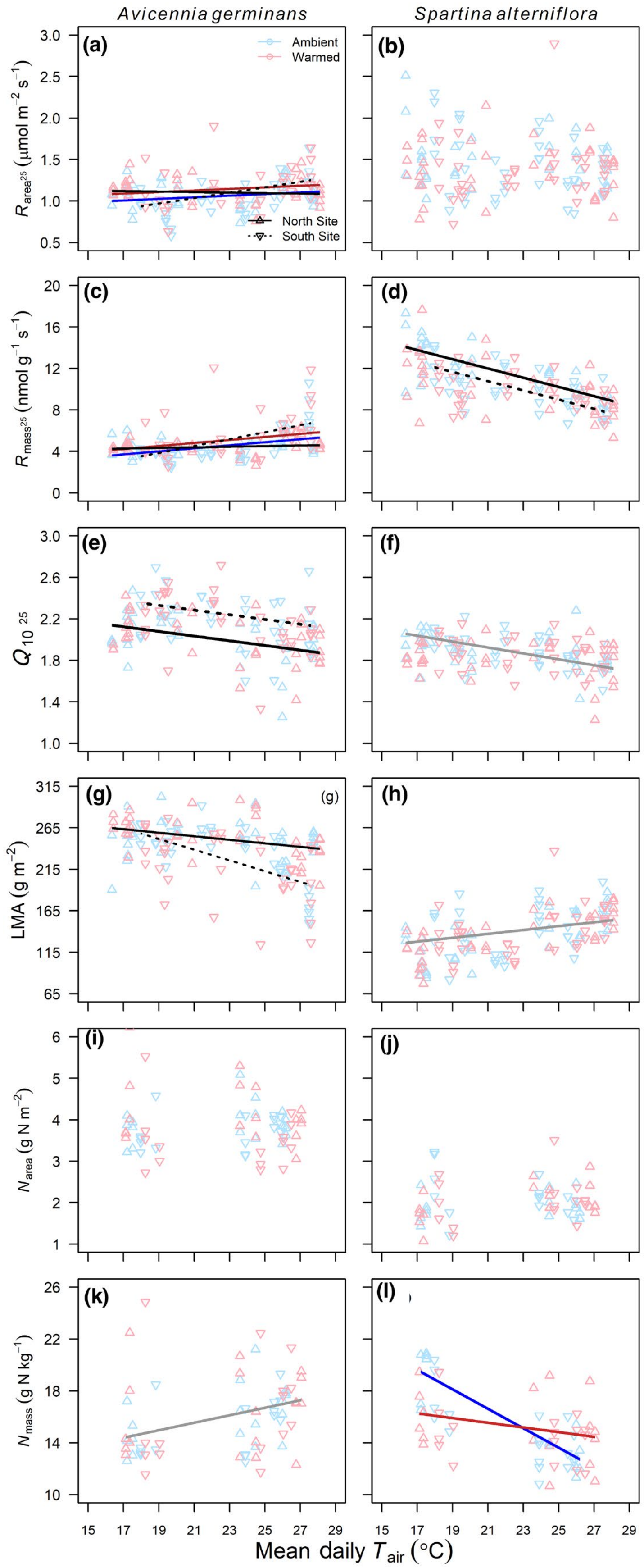

TABLE 2 Analysis of covariance results (*F*-values) testing the relationship between mean daily air temperature (T_{air}) of the preceding 7 days and leaf traits for *Spartina alterniflora* and *Avicennia germinans* and the influence of site and temperature treatment. *F*-values with "*," "**" and "***" are significant at $p < .05$, $p < .01$, and $p < .001$, respectively

Species	Source of variance	R^{25}_{area}	R^{25}_{mass}	Q^{10}_{25}	LMA	N_{mass}	N_{area}
Avicennia germinans	T_{air}	6.23*	26.38***	20.81***	44.62***	5.80*	0.16
	Treatment (*T*)	6.85**	4.94*	0.13	0.98	0.76	0.12
	Site (*S*)	0.24	6.90**	23.80***	23.26***	0.42	9.04**
	$T_{air} \times T$	0.72	0.04	0.14	0.19	0.50	2.84
	$T_{air} \times S$	18.19***	25.24***	0.64	12.08***	0.34	0.03
	$T \times S$	1.44	3.89	0.22	4.62*	0.23	2.84
	$T_{air} \times T \times S$	0.23	0.76	0.35	2.10	0.16	0.01
Spartina alterniflora	T_{air}	1.07	86.88***	14.52***	59.77***	34.93***	0.63
	Treatment (*T*)	1.59	3.02	2.17	0.08	0.06	0.01
	Site (*S*)	0.39	6.18*	1.51	0.51	2.11	1.05
	$T_{air} \times T$	1.06	3.23	2.38	0.05	12.74***	3.65
	$T_{air} \times S$	0.36	2.98	1.69	3.17	0.42	3.31
	$T \times S$	0.11	1.71	1.75	0.43	0.01	0.59
	$T_{air} \times T \times S$	1.24	0.31	1.06	0.50	0.37	0.95

Variable descriptions: R^{25}_{area}, leaf respiration per unit area at 25°C; R^{25}_{mass}, leaf respiration per unit mass at 25°C; Q^{10}_{25}, the temperature sensitivity of leaf *R* at 25°C; LMA, leaf mass per unit area; N_{area}, leaf N per unit area; N_{mass}, leaf N per unit mass.

3.3 | Realized temperature response of *R* and degree of respiratory homeostasis

In *Avicennia*, the realized Q_{10} of R_{area}, which reflects the *long-term* acclimated temperature response of *R*, differed between sites and was 2.01 ± 0.09 at NS and 3.12 ± 0.24 at SS (Figure 3a). The realized Q_{10} of R_{mass} also differed between sites and was 2.25 ± 0.15 at NS and 5.14 ± 0.84 at SS (Figure 3). Realized Q_{10} values did not differ between treatments at either site. These realized Q_{10} values are similar or higher than Q^{10}_{25} estimates (Figure 1). Thus, weak temperature acclimation of *R* in *Avicennia* resulted in little dampening of the temperature sensitivity of realized *R*. Furthermore, the temperature acclimation ratio $Acclim_{homeo}$, which describes the degree of respiratory homeostasis, declined as seasonal temperatures increased indicating a reduction in respiratory homeostasis with larger increases in mean daily T_{air} (Figure 4a,c). The decline in $Acclim_{homeo}$, calculated using in situ estimates of R_{area} and R_{mass}, was consistent across treatments but was more pronounced at SS (R_{area} slope = −0.08 and R_{mass} slope = −0.09) than at NS (R_{area} slope = −0.05 and R_{mass} slope = −0.06; Figure 4a,c).

In *Spartina*, the realized Q_{10} of R_{area} and R_{mass} was 1.79 ± 0.09 and 1.34 ± 0.05, respectively, and was consistent across sites and treatments (Figure 3b,d). These realized Q_{10} values are lower (roughly −10% to −30%) than Q^{10}_{25} estimates, reflecting a dampening of the long-term temperature sensitivity of *R* resulting from both Type II and Type I temperature acclimation. $Acclim_{homeo}$ declined as the change in mean daily T_{air} increased and did so consistently across sites (R_{area} slope = −0.06, R_{mass} slope = −0.03; Figure 4b,d). When $Acclim_{homeo}$ was calculated using in situ estimates of R_{mass}, the decline in $Acclim_{homeo}$ with increasing temperature was lower in *Spartina* than in *Avicennia* (Figure 4c,d). The intercept of the relationship between $Acclim_{homeo}$ and the change in mean daily T_{air} was higher at NS (R_{area} intercept = 1.17 and R_{mass} intercept = 1.09) than at SS (R_{area} intercept = 1.06, R_{mass} intercept = 0.97; Figure 4b,d). We conclude that *Spartina* showed stronger temperature acclimation of *R* and maintained greater homeostasis of realized *R* than *Avicennia*.

3.4 | Leaf N–R relationships

We found that leaf N scaled positively with respiratory capacity in both species. However, in some cases, relationships between leaf N and respiratory capacity depended upon treatment or site (Table 3). In *Avicennia*, R^{25}_{area} increased with N_{area} at SS but not at NS, and R^{25}_{area} at a given N_{area} was higher under warming than ambient conditions (Table 3; Figure 5a). N_{mass} and R^{25}_{mass} scaled positively although the intercept was lower at NS than at SS (Table 3; Figure 5c; Table S4). Overall, N_{area} explained 25% of the variation in R^{25}_{area}, while N_{mass} explained 53% of the variation in R^{25}_{mass} (Table S4).

In *Spartina*, the slope of the N_{area}–R^{25}_{area} relationship was slightly lower at NS than at SS (Table 3; Figure 5b; Table S4). The positive relationship between N_{mass} and R^{25}_{mass} was consistent across treatments and sites (Table 3; Figure 5d; Table S4). N_{area} explained 74% of the variation in R^{25}_{area}, while N_{mass} explained 51% of the variation in R^{25}_{mass} (Table S4). Although temperature acclimation of *R* differed between *Avicennia* and *Spartina*, changes in leaf N explained temperature acclimation patterns in both species.

4 | DISCUSSION

We set out to test whether two contrasting coastal wetland species (*A. germinans* and *S. alterniflora*), individually, show the patterns

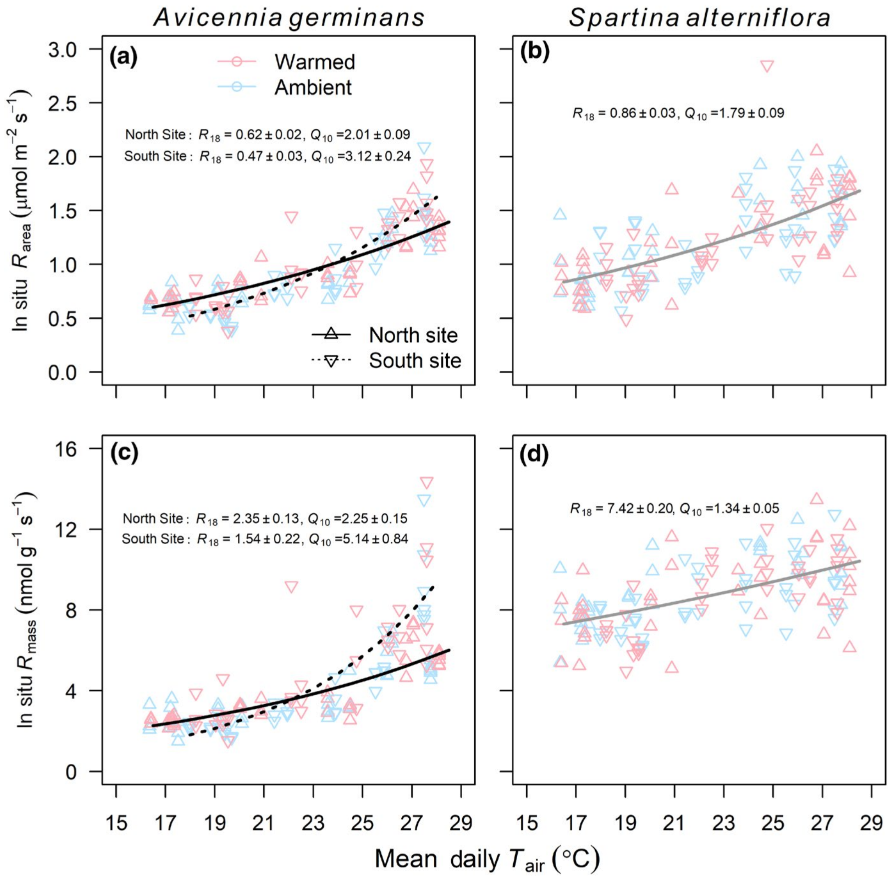

FIGURE 3 The (long-term) response of in situ rates of leaf R (area and mass basis, R_{area}, R_{mass}) to prevailing mean daily air temperature (T_{air}) in *Avicennia germinans* and *Spartina alterniflora* growing at two sites in North Florida (North, South) under two temperature treatments (ambient and warmed). An exponential function that estimates the Q_{10} of R and R at a reference temperature of 18°C (R_{18}) was fit to the data. For each species, we compared Q_{10} estimates and R_{18} between sites and treatments by calculating 95% confidence intervals (standard error × 1.96) of the parameter estimates. When confidence intervals for Q_{10} and R_{18} did not overlap between sites or treatments, we fit separate temperature response functions for each site (solid and dashed lines) or treatment (blue and red lines). If confidence intervals of parameter estimates overlapped, suggesting that parameters were not different between sites or treatments, we fit a single temperature response function across all data (gray lines)

of temperature acclimation of leaf R that are equivalent across seasons, current and warmed climates, and spatially separated sites. In *Avicennia*, we found that R^{25}_{area} and R^{25}_{mass} showed no relationship with prevailing T_{air} at the north site, increased with T_{air} at the south site, and generally increased with experimental warming across both sites. Thus, *Avicennia* showed no evidence for convergent temperature acclimation of respiratory capacity. Even so, Q^{10}_{25} decreased as seasonal temperatures increased and did so consistently across sites and treatments. In *Spartina*, R^{25}_{mass} and Q^{10}_{25} both declined as seasonal temperatures increased. This pattern of seasonal temperature acclimation was largely consistent across sites and treatments supporting our expectation of convergent temperature acclimation. However, our results did not support our hypothesis that temperature acclimation of R would be weaker in *Spartina* (a C_4 species) than in *Avicennia* (a C_3 species). Species differences in temperature acclimation resulted in different degrees of respiratory homeostasis across seasons and treatments, with implications for climate warming impacts on coastal wetland CO_2 fluxes. We conclude that co-occurring species may show contrasting patterns of temperature acclimation. Although temperature acclimation patterns differed between these two dominant coastal wetland plant species, we found that leaf N scaled positively with leaf R in both species, providing an explanation for contrasting patterns of respiratory temperature acclimation that may also inform predictions of temporal or spatial variability in leaf R in coastal wetlands.

There are several possible explanations for the lack of strong temperature acclimation in *Avicennia*. Coastal wetlands are dynamic systems where water levels (i.e., tides) and salinity vary diurnally and seasonally. Salinity depends on proximity to the ocean and freshwater inputs, seasonality of precipitation, and evaporation rates which change with temperature. In our experiment, the southern site (SS) was near an inlet and thus closer to the open ocean while the northern site (NS) was further from the ocean and closer to freshwater inputs. As a result, salinity tends to be higher at SS than at NS (Chapman et al., 2021). Previous work at SS has also indicated that salinity can be very high during summer (up to 60 ppt) and lower during winter (48 ppt) (Dangremond et al., 2020). Previous studies have found small increases in R with increasing salinity, presumably

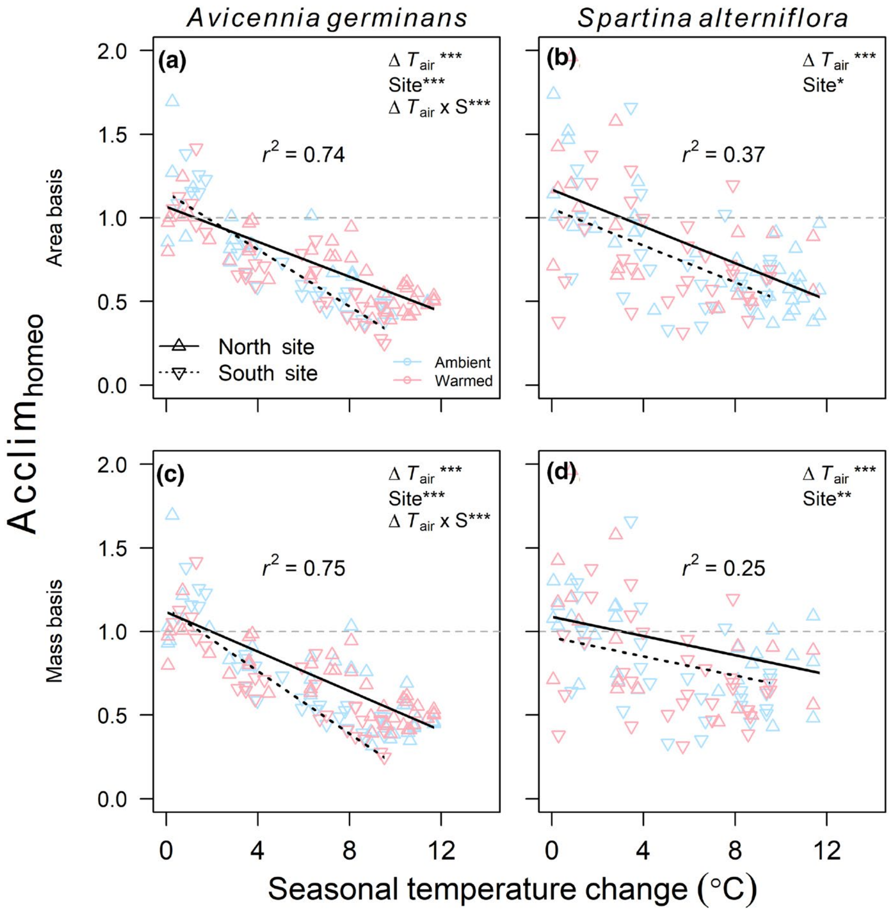

FIGURE 4 The relationship between the ratio describing the degree of respiratory homeostasis over time ($Acclim_{homeo}$ = *R* at lowest mean daily T_{air}/*R* at mean daily T_{air}) and the degree of seasonal temperature change (ΔT_{air} = mean daily T_{air}–lowest mean daily T_{air}) for *Avicennia germinans* and *Spartina alterniflora* growing at two sites in North Florida (North, South) under two temperature treatments (blue = Ambient, red = Warmed). $Acclim_{homeo}$ ratios >1 indicate temperature acclimation resulting in overcompensation (*R* at high T_{air} > *R* at low T_{air}), ratios = 1 indicate temperature acclimation resulting in complete homeostasis, and ratios <1 indicate temperature acclimation resulting in partial homeostasis. Ratios are shown on an area basis (panels a,b) and mass basis (panels c,d). When the intercept or slope of the relationship between $Acclim_{homeo}$ and ΔT_{air} differed between sites, we fit separate lines for each site (solid versus dashed line). Within each panel, the extent to which ΔT_{air}, site, treatment, or their interactions explained variation in $Acclim_{homeo}$ is denoted by asterisks: *, $p < .05$; **, $p < .01$; ***, $p < .001$

due to costs associated with maintaining cellular ion gradients (Aspinwall et al., 2021; Lopez-Hoffman et al., 2007). Thus, the combination of warmer growth temperatures and higher salinity might explain why *R* increased with T_{air} at SS, and why temperature acclimation appeared constrained.

However, averaged across sites, *Avicennia* also increased respiratory capacity in response to experimental warming, suggesting that salinity alone is unlikely to explain the increase in *R* with warmer growth temperatures. Instead, coordination between *R* and photosynthetic capacity might explain the positive relationship between growth temperature and respiratory capacity in *Avicennia*. Importantly, we found that variation in respiratory capacity (e.g., R^{25}_{mass}) over time and across sites and treatments was largely explained by changes in leaf N concentrations. The coupling of leaf N and respiratory capacity could represent enzyme limitation of respiratory capacity (Ryan et al., 1996). However, leaf N and Rubisco carboxylation (V_{cmax}) show a general positive relationship across C_3 species given that a large fraction of N is allocated to Rubisco. A new theory also indicates that temperature acclimation of *R* is consistent with maintenance of "optimal" photosynthetic capacity, where respiratory capacity increases to support processes that maintain photosynthesis (Wang et al., 2020). We hypothesize that respiratory capacity increased with temperature in *Avicennia* due to concomitant changes in photosynthetic capacity, which were reflected in changes in leaf N. If true, *Avicennia* responded to increasing growth temperature by also increasing photosynthetic capacity; a response which is not necessarily consistent with studies of photosynthetic temperature acclimation over space and time (Ali et al., 2015; Way & Sage, 2008; Way & Yamori, 2014).

Temporal patterns in leaf *R* and leaf N in *Avicennia* may have also been influenced by nutrient availability, which could vary with air and soil temperature. Warmer soil and water temperatures during summer may speed up decomposition and N mineralization (Gao et al., 2014; Kirwan & Blum, 2011), which could increase N availability and potentially result in higher leaf N concentrations. Results from a fertilization experiment near our SS have demonstrated that higher N availability leads to higher leaf N concentrations in *Avicennia* (Dangremond et al., 2020; Simpson et al., 2013). Although seasonal changes in N availability were not quantified in our study, we found that leaf N concentrations increased in *Avicennia* with prevailing air temperature across both sites. Therefore, higher N availability during warmer time periods may have resulted in higher leaf N, greater photosynthetic capacity, and coordinated increases in respiratory capacity in *Avicennia* (Wang et al., 2020).

Although respiratory capacity increased with growth temperature in *Avicennia*, indicating no Type II temperature acclimation, we observed a decline in the short-term Q_{10} of R as prevailing T_{air} increased across seasons (i.e., Type I acclimation, Atkin & Tjoelker, 2003; Slot & Kitajima, 2015). This acclimation response is less common but has been observed in several studies (Atkin et al., 2000; Ow et al., 2010; Zaragoza-Castells et al., 2007). Mechanisms of Type I acclimation are unclear although regulatory changes in respiratory enzymes could be involved (Atkin et al., 2005; Kruse et al., 2011, 2020). Other studies have identified positive relationships between soluble sugars and the Q_{10} of R (Azcón-Bieto et al., 1983; Ow et al., 2010) which could reflect substrate limitation of the maximum catalytic enzyme activity (Atkin & Tjoelker, 2003). It is possible that high respiratory demand during summer may have reduced soluble sugar concentrations which in turn reduced maximum catalytic activity and the temperature sensitivity of R.

The complexity of C_4 photosynthesis has been hypothesized to come at the cost of reduced phenotypic plasticity or lower temperature acclimation capacity in C_4 plants (Sage & McKown, 2006; Yamori et al., 2014). Yet, experimental work has found no clear

TABLE 3 Analysis of covariance results (F-values) testing relationships between leaf nitrogen concentrations (area and mass basis; N_{area}, N_{mass}) and leaf respiration at 25°C (area and mass basis, R^{25}_{area}, R^{25}_{mass}) in *Avicennia germinans* and *Spartina alterniflora*. F-values with "*," "**," and "***" are significant at $p < .05$, $p < .01$, and $p < .001$, respectively

Source of variance	*Avicennia germinans*	*Spartina alterniflora*
Response variable = R^{25}_{area}		
N_{area}	5.77*	154.20***
Treatment (T)	4.18*	2.59
Site (S)	0.17	0.00
$N_{area} \times T$	0.02	0.21
$N_{area} \times S$	7.54**	5.41*
$T \times S$	1.37	2.06
$N_{area} \times T \times S$	0.30	0.20
Response variable = R^{25}_{mass}		
N_{mass}	50.73***	51.25***
Treatment (T)	3.47	3.10
Site (S)	4.51*	0.82
$N_{mass} \times T$	0.36	0.03
$N_{mass} \times S$	3.24	0.82
$T \times S$	3.47	3.46
$N_{mass} \times T \times S$	0.63	0.41

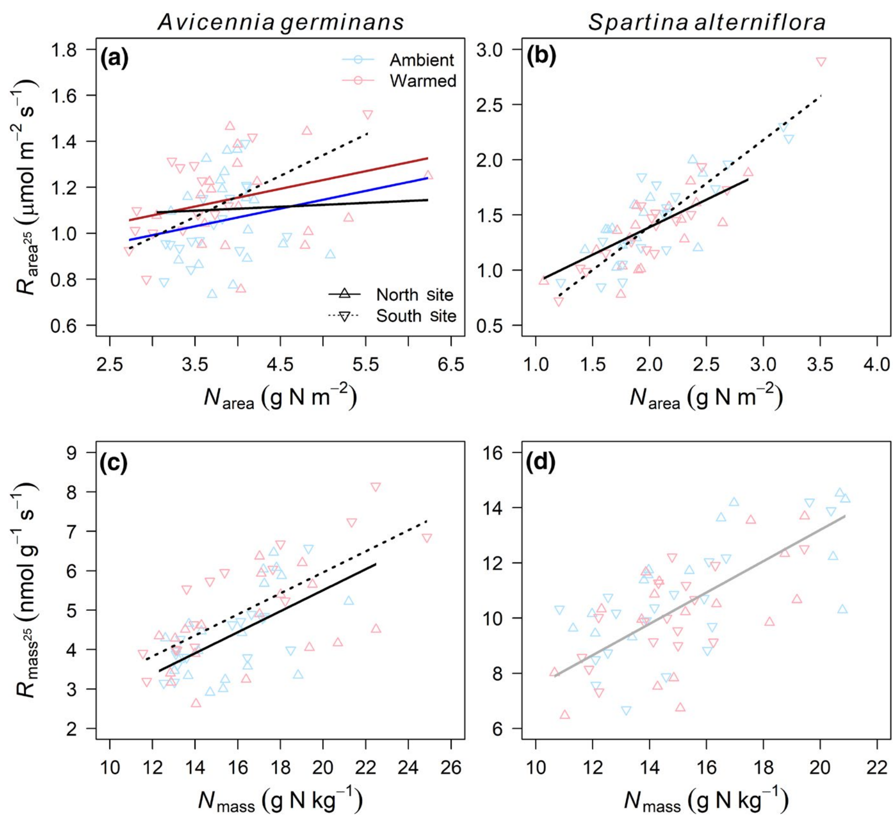

FIGURE 5 The relationship between leaf N concentrations (area and mass basis; N_{area}, N_{mass}) and leaf respiration at 25°C (area and mass basis; R^{25}_{area}, R^{25}_{mass}) in *Avicennia germinans* (panels a, c) and *Spartina alterniflora* growing at two sites in North Florida (North, South) under two temperature treatments (blue = ambient, red = warmed). Gray solid lines signify a common relationship across sites and treatments. Black solid and dashed lines signify different relationships between sites. Red and blue lines signify different relationships between treatments that are consistent across sites. Intercept and slope parameters and model coefficients of variation (R^2) are provided in Table S4

differences in temperature acclimation responses between C_3 and C_4 plant species (Smith & Dukes, 2017). We tested the hypothesis that *Spartina* would show weaker temperature acclimation than *Avicennia* and found no support for this expectation. In fact, we found that *Spartina* reduced R^{25}_{mass} and the short-term Q_{10} of R as growth temperatures increased (Type II acclimation and Type I acclimation) over time and across sites and treatments while *Avicennia* generally showed *increased* respiratory capacity with temperature. The temperature acclimation results in *Spartina* are similar to results from other studies with tree species representing different biomes (Aspinwall et al., 2016; Reich et al., 2016). We conclude that *Spartina*, a dominant C_4 marsh grass, showed rather consistent temperature acclimation of R over space and time, and with climate warming, which could reduce the temperature sensitivity of CO_2 fluxes in marsh-dominated coastal wetlands.

Convergent temperature acclimation in *Spartina* could be partly influenced by the modest warming created by our passive warming chambers. The chambers increased mean daily T_{air} 0.6–0.7°C and maximum daily T_{air} ~3°C. At the same sites, Chapman et al., (2021) found the chambers increased mean daytime T_{air} 1.6°C. For context, average T_{air} across the contiguous United States has increased 0.7°C since the 1960s, with additional warming of ~1.4°C expected over the next few decades (USGCRP, 2018). A similar amount of warming is expected in the southeast United States (Ashfaq et al., 2016). Therefore, the warming created by the chambers is within the range of warming expected over the next few decades. Moreover, warming increased respiratory capacity of *Avicennia*, indicating that the warming treatment was sufficient to alter biological processes.

Local adaptation or temperature seasonality across the species range could have contributed to differences in temperature acclimation between species. The location of our experiment is near the southern (warm) limit of *Spartina* and the northern (cool) limit of *Avicennia* on the Atlantic coast. Both species have shown evidence of local adaptation and may possess traits that influence their acclimation capacity (Cook-Patton et al., 2015; Kennedy et al., 2020; Kirwan et al., 2009; Markley et al., 1982; Osland et al., 2020). However, robust temperature acclimation in *Spartina* might be explained by the relatively high temperature seasonality across the species range. Weaker temperature acclimation in *Avicennia* might be consistent with less temperature seasonality across the species range. Nonetheless, studies that have compared acclimation responses among species from more- or less-seasonal climates have found no clear differences (Reich et al., 2016; Scafaro et al., 2017). Additional studies would be required to understand the potential influence of local adaptation or species climatic niche on temperature acclimation responses in coastal plants.

Repeated measurements of the short-term temperature response of R provided a powerful approach for examining the consequence of species differences in temperature acclimation. Using individual temperature response measurements to estimate realized (in situ) R, we found that the Q_{10} of realized R was similar to the short-term Q_{10} of R in *Avicennia*. In *Avicennia*, we also found that the ratio describing the degree of respiratory homeostasis ($Acclim_{homeo}$) declined quickly with larger increases in growth temperature indicating that Type I acclimation alone was not sufficient to dampen the temperature sensitivity of realized R and resulted in reduced homeostasis of R. In *Spartina*, the Q_{10} of realized R was lower than the short-term Q_{10}. Moreover, $Acclim_{homeo}$ declined more slowly with larger increases in T_{air}, especially when $Acclim_{homeo}$ was calculated using estimates of in situ R_{mass}. Thus, Type II and Type I acclimation in *Spartina* resulted in greater homeostasis of R. Our results agree with the synthesis of Slot and Kitajima (2015), who found that Type II acclimation results in greater homeostasis of R than Type I acclimation alone.

Although species differed in temperature acclimation of R, leaf N explained temporal and spatial variation in respiratory capacity in both species. Species differences in leaf N and R over time may be partly related to different nutrient acquisition or investment strategies. For instance, *Avicennia* is an evergreen species and is known to be very responsive to N availability (Dangremond et al., 2020; Simpson et al., 2013). In our study, *Avicennia* decreased LMA and increased leaf N as seasonal temperatures increased. Some studies have shown that *Spartina* is also responsive to nutrients (e.g., Mendelssohn, 1979), although responses are variable among individual studies (e.g., Weaver & Armitage, 2020). However, *Spartina* exhibits a strong seasonality to leaf development and leaf N concentrations; as seasonal temperatures increase LMA increases and leaf N decreases. These distinct seasonal patterns could explain the contrasting seasonal responses of respiratory capacity, but the close coupling of leaf N and R in both species.

More broadly, our results indicate that leaf N may be a useful predictor of foliar C fluxes in dominant coastal wetland species, just as leaf N is used to estimate leaf R in land surface models that predict terrestrial C fluxes over space and time (Atkin et al., 2015; Fisher et al., 2014; Lawrence et al., 2019). In fact, in our species and across our sites, leaf N explained more variation in leaf R than prevailing T_{air}. We note that coastal wetlands are not well-represented in land surface models due to gaps in our understanding of key processes and data limitations (Ward et al., 2020). The data presented here could improve representation and parameterization of CO_2 exchange between coastal vegetation and the atmosphere in large-scale models.

Our results indicate that patterns of respiratory temperature acclimation may differ between co-occurring coastal wetland species representing different functional types. Convergent acclimation responses may be expected in some but not all species. Although acclimation patterns may differ among species, leaf N may be a useful predictor of respiratory capacity, and ultimately respiratory C fluxes across a range of growth temperatures. The data presented here will be particularly useful for improving predictions of C fluxes from coastal wetlands under current and future climate conditions. Nonetheless, studies that examine coordination of leaf respiratory and photosynthetic capacity over temporal and spatial gradients will provide further insight into aboveground physiological controls of coastal wetland C cycling.

ACKNOWLEDGMENTS

This work was funded by NSF DEB 1655659 awarded to SKC. Support for MJA and JC was provided by USDA-NIFA award 2019-67013-29161, the University of North Florida, and Auburn University. Additional support for MAS was provided by the Garden Club of America Award in Coastal Wetlands Studies. The authors thank GTMNERR staff and volunteers for their support and assistance with this experiment.

CONFLICT OF INTEREST

The authors have no conflicts of interest to declare.

AUTHOR CONTRIBUTIONS

SKC, MAS, and MJA conceived and designed the experiment. MAS and GC collected the data. MAS, JC, and MJA analyzed the data. MAS and MJA wrote the manuscript with input from all authors.

DATA AVAILABILITY STATEMENT

All data used in this manuscript are publicly available and can be accessed at https://doi.org/10.5281/zenodo.5567749.

ORCID

Jeff Chieppa https://orcid.org/0000-0003-2854-1514

Michael J. Aspinwall https://orcid.org/0000-0003-0199-2972

REFERENCES

Akaji, Y., Inoue, T., Tomimatsu, H., & Kawanishi, A. (2019). Photosynthesis, respiration, and growth patterns of *Rhizophora stylosa* seedlings in relation to growth temperature. *Trees*, *33*, 1041–1049. https://doi.org/10.1007/s00468-019-01840-7

Ali, A. A., Xu, C. G., Rogers, A., McDowell, N. G., Medlyn, B. E., Fisher, R. A., Wullschleger, S. D., Reich, P. B., Vrugt, J. A., Bauerle, W. L., Santiago, L. S., & Wilson, C. J. (2015). Global-scale environmental control of plant photosynthetic capacity. *Ecological Applications*, *25*, 2349–2365. https://doi.org/10.1890/14-2111.1

Alongi, D. M. (2020). Carbon balance in salt marsh and mangrove ecosystems: A global synthesis. *Journal of Marine Science and Engineering*, *8*(10), 767. https://doi.org/10.3390/jmse8100767

Ashfaq, M., Rastogi, D., Mei, R., Kao, S.-C., Grangrade, S., Naz, B., & Touma, D. (2016). High-resolution ensemble projections of near-term regional climate over the continental United States. *Journal of Geophysical Research: Atmospheres*, *121*(17), 9943–9963. https://doi.org/10.1002/2016JD025285

Aspinwall, M. J., Drake, J. E., Campany, C., Vårhammar, A., Ghannoum, O., Tissue, D. T., Reich, P. B., & Tjoelker, M. G. (2016). Convergent acclimation of leaf photosynthesis and respiration to prevailing ambient temperatures under current and warmer climates in *Eucalyptus tereticornis*. *New Phytologist*, *212*, 354–367.

Aspinwall, M. J., Faciane, M., Harris, K., O'Toole, M., Neece, A., Jerome, V., Colón, M., Chieppa, J., & Feller, I. C. (2021). Salinity has little effect on photosynthetic and respiratory responses to seasonal temperature changes in black mangrove (*Avicennia germinans*) seedlings. *Tree Physiology*, *41*(1), 103–118.

Aspinwall, M. J., Pfautsch, S., Tjoelker, M. G., Vårhammar, A., Possell, M., Drake, J. E., Reich, P. B., Tissue, D. T., Atkin, O. K., Rymer, P. D., & Dennison, S. (2019). Range size and growth temperature influence Eucalyptus species responses to an experimental heatwave. *Global Change Biology*, *25*, 1665–1684.

Aspinwall, M., Vårhammar, A., Blackman, C., Tjoelker, M., Ahrens, C., Byrne, M., Tissue, D. T., & Rymer, P. (2017). Adaptation and acclimation both influence photosynthetic and respiratory temperature responses in *Corymbia calophylla*. *Tree Physiology*, *37*(8), 1095–1112. https://doi.org/10.1093/treephys/tpx047

Atkin, O. K., Bloomfield, K. J., Reich, P. B., Tjoelker, M. G., Asner, G. P., Bonal, D., Bönisch, G., Bradford, M. G., Cernusak, L. A., Cosio, E. G., Creek, D., Crous, K. Y., Domingues, T. F., Dukes, J. S., Egerton, J. J. G., Evans, J. R., Farquhar, G. D., Fyllas, N. M., Gauthier, P. P. G., … Zaragoza-Castells, J. (2015). Global variability in leaf respiration in relation to climate, plant functional types and leaf traits. *New Phytologist*, *206*, 614–636. https://doi.org/10.1111/nph.13253

Atkin, O. K., Bruhn, D., Hurry, V. M., & Tjoelker, M. G. (2005). Evans Review No. 2: The hot and the cold: Unravelling the variable response of plant respiration to temperature. *Functional Plant Biology*, *32*, 87–105. https://doi.org/10.1071/FP03176

Atkin, O. K., Evans, J. R., Ball, M. C., Lambers, H., & Pons, T. L. (2000). Leaf respiration of snow gum in the light and dark. Interactions between temperature and irradiance. *Plant Physiology*, *122*, 915–923. https://doi.org/10.1104/pp.122.3.915

Atkin, O. K., Meir, P., & Turnbull, M. H. (2014). Improving representation of leaf respiration in large-scale predictive climate-vegetation models. *New Phytologist*, *202*(3), 743–748. https://doi.org/10.1111/nph.12686

Atkin, O. K., Scheurwater, I., & Pons, T. L. (2007). Respiration as a percentage of daily photosynthesis in whole plants is homeostatic at moderate, but not high, growth temperatures. *New Phytologist*, *174*, 367–380. https://doi.org/10.1111/j.1469-8137.2007.02011.x

Atkin, O. K., & Tjoelker, M. G. (2003). Thermal acclimation and the dynamic response of plant respiration to temperature. *Trends in Plant Science*, *8*, 343–351. https://doi.org/10.1016/S1360-1385(03)00136-5

Azcón-Bieto, J., Lambers, H., & Day, D. A. (1983). Effect of photosynthesis and carbohydrate status on respiratory rates and the involvement of the alternative pathway in leaf respiration. *Plant Physiology*, *72*, 598–603. https://doi.org/10.1104/pp.72.3.598

Bolstad, P. V., Reich, P. B., & Lee, T. (2003). Rapid temperature acclimation of leaf respiration rates in *Quercus alba* and *Quercus rubra*. *Tree Physiology*, *23*(14), 969–976. https://doi.org/10.1093/treephys/23.14.969

Bouillon, S., Borges, A. V., Castañeda-Moya, E., Diele, K., Dittmar, T., Duke, N. C., Kristensen, E., Lee, S. Y., Marchand, C., Middelburg, J. J., Rivera-Monroy, V. H., Smith, T. J., & Twilley, R. R. (2008). Mangrove production and carbon sinks: A revision of global budget estimates. *Global Biogeochemical Cycles*, *22*(2). https://doi.org/10.1029/2007GB003052

Bruhn, D., Egerton, J. J. G., Loveys, B. R., & Ball, M. C. (2007). Evergreen leaf respiration acclimates to long-term nocturnal warming under field conditions. *Global Change Biology*, *13*, 1216–1223. https://doi.org/10.1111/j.1365-2486.2007.01351.x

Chapman, S. K., Feller, I. C., Canas, G., Hayes, M. A., Dix, N., Hester, M., Morris, J., & Langley, J. A. (2021). Mangrove growth response to experimental warming is greatest near the range limit in northeast Florida. *Ecology*, *10*(6). https://doi.org/10.1002/ecy.3320

Cheesman, A. W., & Winter, K. (2013). Growth response and acclimation of CO_2 exchange characteristics to elevated temperatures in tropical tree seedlings. *Journal of Experimental Botany*, *64*, 3817–3828. https://doi.org/10.1093/jxb/ert211

Cook-Patton, S. C., Lehmann, M., & Parker, J. D. (2015). Convergence of three mangrove species towards freeze-tolerant phenotypes at an expanding range edge. *Functional Ecology*, *29*, 1332–1340. https://doi.org/10.1111/1365-2435.12443

Crous, K. Y., Wallin, G., Atkin, O. K., Uddling, J., & af Ekenstam, A. (2017). Acclimation of light and dark respiration to experimental and seasonal warming are mediated by changes in leaf nitrogen in *Eucalyptus globulus*. *Tree Physiology*, *37*(8), 1069–1083. https://doi.org/10.1093/treephys/tpx052

Dangremond, E. M., Simpson, L. T., Osborne, T. Z., & Feller, I. C. (2020). Nitrogen enrichment accelerates mangrove range expansion in the temperate-tropical ecotone. *Ecosystems*, *23*, 703–714. https://doi.org/10.1007/s10021-019-00441-2

De Boeck, H. J., De Groote, T., & Nijs, I. (2012). Leaf temperatures in glasshouses and open-top chambers. *New Phytologist*, *194*, 1155–1164. https://doi.org/10.1111/j.1469-8137.2012.04117.x

Dix, N., Brockmeyer, R., Chapman, S., Angelini, C., Kidd, S., Eastman, S., & Radabaugh, K. R. (2021). Northeast Florida. In K. R. Radabaugh, C. E. Powell, & R. P. Moyer (Eds.), *Coastal habitat integrated mapping and monitoring program report for the State of Florida*. Florida Fish and Wildlife Conservation Commission Fish and Wildlife Research Institute Technical Report No. 21.

Donato, D., Kauffman, J., Murdiyarso, D., Kurnianto, S., Stidham, M., & Kanninen, M. (2011). Mangroves among the most carbon-rich forests in the tropics. *Nature Geoscience*, *4*, 293–297. https://doi.org/10.1038/ngeo1123

Drake, J. E., Aspinwall, M. J., Pfautsch, S., Rymer, P. D., Reich, P. B., Smith, R. A., Crous, K. Y., Tissue, D. T., Ghannoum, O., & Tjoelker, M. G. (2015). The capacity to cope with climate warming declines from temperate to tropical latitudes in two widely distributed Eucalyptus species. *Global Change Biology*, *21*, 459–472.

Evans, J. R. (1989). Photosynthesis and nitrogen relationships in leaves of C_3 plants. *Oecologia*, *78*, 9–19. https://doi.org/10.1007/BF00377192

Feng, T., Zhang, L., Chen, Q., Ma, Z., Wang, H., Shangguan, Z., Wang, L., & He, J.-S. (2021). Dew formation reduction in global warming experiments and the potential consequences. *Journal of Hydrology*, *593*, 125819. https://doi.org/10.1016/j.jhydrol.2020.125819

Fisher, J. B., Huntzinger, D. N., Schwalm, C. R., & Sitch, S. (2014). Modeling the terrestrial biosphere. *Annual Review of Environment and Resources*, *39*, 91–123. https://doi.org/10.1146/annurev-environ-012913-093456

Gao, H., Bai, J., He, X., Zhao, Q., Lu, Q., & Wang, J. (2014). High temperature and salinity enhance soil nitrogen mineralization in a tidal freshwater marsh. *PLoS One*, *9*(4). https://doi.org/10.1371/journal.pone.0095011

Ghannoum, O., Evans, J. R., Chow, W. S., Andrews, T. J., Conroy, J. P., & von Caemmerer, S. (2005). Faster Rubisco is the key to superior nitrogen-use efficiency in NADP-malic enzyme relative to NAD-malic enzyme C_4 grasses. *Plant Physiology*, *137*, 638–650. https://doi.org/10.1104/pp.104.054759

Heskel, M. A., O'Sullivan, O. S., Reich, P. B., Tjoelker, M. G., Weerasinghe, L. K., Penillard, A., Egerton, J. J. G., Creek, D., Bloomfield, K. J., Xiang, J., Sinca, F., Stangl, Z. R., Torre, A. M., Griffin, K. L., Huntingford, C., Hurry, V., Meir, P., Turnbull, M. H., & Atkin, O. K. (2016). Convergence in the temperature response of leaf respiration across biomes and plant functional types. *Proceedings of the National Academy of Sciences of the United States of America*, *113*(14), 3832–3837. https://doi.org/10.1073/pnas.1520282113

Hikosaka, K., & Shigeno, A. (2009). The role of Rubisco and cell walls in the interspecific variation in photosynthetic capacity. *Oecologia*, *160*, 443–451. https://doi.org/10.1007/s00442-009-1315-z

Kennedy, J. P., Preziosi, R. F., Rowntree, J. K., & Feller, I. C. (2020). Is the central-marginal hypothesis a general rule? Evidence from three distributions of an expanding mangrove species, *Avicennia germinans* (L.) L. *Molecular Ecology*, *29*, 704–719.

King, A. W., Gunderson, C. A., Post, W. M., Weston, D. J., & Wullschleger, S. D. (2006). Plant respiration in a warmer world. *Science*, *312*, 536–537. https://doi.org/10.1126/science.1114166

Kirwan, M. L., & Blum, L. K. (2011). Enhanced decomposition offsets enhanced productivity and soil carbon accumulation in coastal wetlands responding to climate change. *Biogeosciences*, *8*, 987–993. https://doi.org/10.5194/bg-8-987-2011

Kirwan, M. L., Guntenspergen, G. R., & Morris, J. T. (2009). Latitudinal trends in *Spartina alterniflora* productivity and the response of coastal marshes to global change. *Global Change Biology*, *15*(8), 1982–1989.

Kruse, J., Rennenberg, H., & Adams, M. A. (2011). Steps towards a mechanistic understanding of respiratory temperature responses. *New Phytologist*, *189*, 659–677. https://doi.org/10.1111/j.1469-8137.2010.03576.x

Kruse, J., Turnbull, T., Rennenberg, H., & Adams, M. A. (2020). Plasticity of leaf respiratory and photosynthetic traits in *Eucalyptus grandis* and *E. regnans* grown under variable light and nitrogen availability. *Frontiers in Forests and Global Change*. https://doi.org/10.3389/ffgc.2020.00005

Lawrence, D. M., Fisher, R. A., Koven, C. D., Oleson, K. W., Swenson, S. C., Bonan, G., Collier, N., Ghimire, B., Kampenhout, L., Kennedy, D., Kluzek, E., Lawrence, P. J., Li, F., Li, H., Lombardozzi, D., Riley, W. J., Sacks, W. J., Shi, M., Vertenstein, M., … Zeng, X. (2019). The community land model version 5: Description of new features, benchmarking, and impact of forcing uncertainty. *Journal of Advances in Modeling Earth Systems*, *11*, 4245–4287. https://doi.org/10.1029/2018MS001583

Lee, T. D., Reich, P. B., & Bolstad, P. V. (2005). Acclimation of leaf respiration to temperature is rapid and related to specific leaf area, soluble sugars and leaf nitrogen across three temperate deciduous tree species. *Functional Ecology*, *19*, 640–647. https://doi.org/10.1111/j.1365-2435.2005.01023.x

Lloyd, J., & Taylor, J. (1994). On the temperature dependence of soil respiration. *Functional Ecology*, *8*(3), 315–323. https://doi.org/10.2307/2389824

Lombardozzi, D., Bonan, G., Smith, N. G., Dukes, J. S., & Fisher, R. (2015). Temperature acclimation of photosynthesis and respiration: A key uncertainty in the carbon cycle–climate feedback. *Geophysical Research Letters*, *42*, 8624–8631. https://doi.org/10.1002/2015GL065934

Lopez-Hoffman, L., Anten, N. P. R., Martinez-Ramos, M., & Ackerly, D. D. (2007). Salinity and light interactively affect neotropical mangrove seedlings at the leaf and whole plant levels. *Oecologia*, *150*, 545–556. https://doi.org/10.1007/s00442-006-0563-4

Lu, W., Xiao, J., Liu, F., Zhang, Y., Liu, C., & Lin, G. (2017). Contrasting ecosystem CO_2 fluxes of inland and coastal wetlands: A meta-analysis of eddy covariance data. *Global Change Biology*, *23*(3), 1180–1198.

Lugo, A. E., Brown, S. L., Dodson, R., Smith, T. S., & Shugart, H. H. (1999). The Holdridge life zones of the conterminous United States in relation to ecosystem mapping. *Journal of Biogeography*, *26*, 1025–1038. https://doi.org/10.1046/j.1365-2699.1999.00329.x

Lugo, A. E., & Snedaker, S. C. (1974). The ecology of mangroves. *Annual Review of Ecology and Systematics*, *5*, 39–64. https://doi.org/10.1146/annurev.es.05.110174.000351

Markley, C., McMillan, G. A., & Thompson, G. A. Jr. (1982). Latitudinal differentiation in response to chilling temperatures among populations of three mangroves, *Avicennia germinans*, *Laguncularia racemosa*, and *Rhizophora mangle*, from the western tropical Atlantic and Pacific Panama. *Canadian Journal of Botany*, *60*, 2704–2715.

Mcleod, E., Chmura, G. L., Bouillon, S., Salm, R., Björk, M., Duarte, C. M., Lovelock, C. E., Schlesinger, W. H., & Silliman, B. R. (2011). A blueprint for blue carbon: Toward an improved understanding of the role of vegetated coastal habitats in sequestering CO_2. *Frontiers in Ecology and the Environment*, *9*(10), 552–560.

Mendelssohn, I. A. (1979). The influence of nitrogen level, form, and application method on the growth response of *Spartina alterniflora* in North Carolina. *Estuaries*, *2*, 106–112. https://doi.org/10.2307/1351634

NOAA. National Climate Data Center website. Retrieved February 4, 2020, Available from https://www.ncdc.noaa.gov/cdo-web/webservices

O'Leary, B. M., Asao, S., Millar, A. H., & Atkin, O. K. (2019). Core principles which explain variation in respiration across biological scales. *New Phytologist*, *222*(2), 670–686. https://doi.org/10.1111/nph.15576

Osland, M. J., Day, R. H., Hall, C. T., Feher, L. C., Armitage, A. R., Cebrian, J., Dunton, K. H., Hughes, A. R., Kaplan, D. A., Langston, A. K., Macy, A., Weaver, C. A., Anderson, G. H., Cummins, K., & Feller, I. C. (2020). Temperature thresholds for black mangrove (*Avicennia germinans*) freeze damage, mortality and recovery in North America: Refining tipping points for range expansion in a warming climate. *Journal of Ecology*, *108*, 654–665.

O'sullivan, O. S., Heskel, M. A., Reich, P. B., Tjoelker, M. G., Weerasinghe, L. K., Penillard, A., Zhu, L., Egerton, J. J. G., Bloomfield, K. J., Creek, D., Bahar, N. H. A., Griffin, K. L., Hurry, V., Meir, P., Turnbull, M. H., & Atkin, O. K. (2017). Thermal limits of leaf metabolism across biomes. *Global Change Biology*, *23*, 209–223. https://doi.org/10.1111/gcb.13477

O'Sullivan, O. S., Weerasinghe, K. W., Evans, J. R., Egerton, J. J., Tjoelker, M. G., & Atkin, O. K. (2013). High-resolution temperature responses of leaf respiration in snow gum (*Eucalyptus pauciflora*) reveal high-temperature limits to respiratory function. *Plant, Cell & Environment*, *36*, 1268–1284.

Ow, L. F., Whitehead, D., Walcroft, A. S., & Turnbull, M. H. (2008). Thermal acclimation of respiration but not photosynthesis in *Pinus radiata*. *Functional Plant Biology*, *35*, 448–461. https://doi.org/10.1071/FP08104

Ow, L. F., Whitehead, D., Walcroft, A. S., & Turnbull, M. H. (2010). Seasonal variation in foliar carbon exchange in *Pinus radiate* and *Populus deltoides*: Respiration acclimates fully to changes in temperature but photosynthesis does not. *Global Change Biology*, *16*, 288–302.

Patterson, A. E., Arkebauer, R., Quallo, C., Heskel, M. A., Li, X., Boelman, N., & Griffin, K. L. (2018). Temperature response of respiration and respiratory quotients of 16 co-occurring temperate tree species. *Tree Physiology*, *38*, 1319–1332. https://doi.org/10.1093/treephys/tpx176

Piao, S., Sitch, S., Ciais, P., Friedlingstein, P., Peylin, P., Wang, X., Ahlström, A., Anav, A., Canadell, J. G., Cong, N., Huntingford, C., Jung, M., Levis, S., Levy, P. E., Li, J., Lin, X., Lomas, M. R., Meng, L., Luo, Y., … Zeng, N. (2013). Evaluation of terrestrial carbon cycle models for their response to climate variability and to CO_2 trends. *Global Change Biology*, *19*, 2117–2132.

R Core Team. (2013). *R: A language and environment for statistical computing*. R Foundation for Statistical Computing.

Reich, P. B., Sendall, K. M., Stefanski, A., Wei, X., Rich, R. L., & Montgomery, R. A. (2016). Boreal and temperate trees show strong acclimation of respiration to warming. *Nature*, *531*, 633–636. https://doi.org/10.1038/nature17142

Reich, P. B., Tjoelker, M. G., Pregitzer, K. S., Wright, I. J., Oleksyn, J., & Machado, J. L. (2008). Scaling of respiration to nitrogen in leaves, stems and roots of higher land plants. *Ecology Letters*, *11*, 793–801. https://doi.org/10.1111/j.1461-0248.2008.01185.x

Ryan, M. G. (1991). Effects of climate change on plant respiration. *Ecological Applications*, *1*(2), 157–167. https://doi.org/10.2307/1941808

Ryan, M. G., Hubbard, R. M., Pongracic, S., Raison, R. J., & McMurtrie, R. E. (1996). Foliage, fine-root, woody-tissue and stand respiration in *Pinus radiata* in relation to nitrogen status. *Tree Physiology*, *16*(3), 333–343. https://doi.org/10.1093/treephys/16.3.333

Sage, R. F., & McKown, A. D. (2006). Is C_4 photosynthesis less phenotypically plastic than C_3 photosynthesis? *Journal of Experimental Botany*, *57*, 303–317. https://doi.org/10.1093/jxb/erj040

Scafaro, A. P., Xiang, S., Long, B. M., Bahar, N. H. A., Weerasinghe, L. K., Creek, D., Evans, J. R., Reich, P. B., & Atkin, O. K. (2017). Strong thermal acclimation of photosynthesis in tropical and temperate wet-forest tree species: The importance of altered Rubisco content. *Global Change Biology*, *23*, 2783–2800. https://doi.org/10.1111/gcb.13566

Simpson, L. T., Feller, I. C., & Chapman, S. K. (2013). Effects of competition and nutrient enrichment on *Avicennia germinans* in the salt marsh-mangrove ecotone. *Aquatic Botany*, *104*, 55–59.

Slot, M., & Kitajima, K. (2015). General patterns of acclimation of leaf respiration to warmer temperatures across biomes and plant types. *Oecologia*, *177*, 885–900.

Smith, N. G., & Dukes, J. S. (2013). Plant respiration and photosynthesis in global-scale models: Incorporating acclimation to temperature and CO_2. *Global Change Biology*, *19*, 45–63.

Smith, N. G., & Dukes, J. S. (2017). Short-term acclimation to warmer temperatures accelerates leaf carbon exchange processes across plant types. *Global Change Biology*, *23*, 4840–4853. https://doi.org/10.1111/gcb.13735

Smith, N. G., Malyshev, S., Shevliakova, E., Kattge, J., & Dukes, J. S. (2016). Foliar temperature acclimation reduces simulated carbon sensitivity to climate. *Nature Climate Change*, *6*, 407–411. https://doi.org/10.1038/nclimate2878

Smith, N. G., McNellis, R., & Dukes, J. S. (2020). No acclimation: Instantaneous responses to temperature maintain homeostatic photosynthetic rates under experimental warming across a precipitation gradient in *Ulmus americana*. *Annals of Botany- Plants*, *12*(4). https://doi.org/10.1093/aobpla/plaa027

Tjoelker, M. G., Oleksyn, J., Lorenc-Plucinska, G., & Reich, P. B. (2009). Acclimation of respiratory temperature responses in northern and southern populations of *Pinus banksiana*. *New Phytologist*, *181*, 218–229.

Tjoelker, M. G., Oleksyn, J., & Reich, P. B. (1999). Acclimation of respiration to temperature and CO_2 in seedlings of boreal tree species in relation to plant size and relative growth rate. *Global Change Biology*, *5*, 679–691.

Tjoelker, M. G., Oleksyn, J., Reich, P. B., & Zytkowiak, R. (2008). Coupling of respiration, nitrogen, and sugars underlies convergent temperature acclimation in *Pinus banksiana* across wide-ranging sites and populations. *Global Change Biology*, *14*, 782–797.

USGCRP. (2018). Impacts, risks, and adaptation in the United States: Fourth National Climate Assessment, Volume II. In D. R. Reidmiller, C. W. Avery, D. R. Easterling, K. E. Kunkel, K. L. M. Lewis, T. K. Maycock, & B. C. Stewart (Eds.) U.S. Global Change Research Program. Washington, DC, USA. 1515 pp.

Vanderwel, M. C., Slot, M., Lichstein, J. W., Reich, P. B., Kattge, J., Atkin, O. K., Bloomfield, K. J., Tjoelker, M. G., & Kitajima, K. (2015). Global convergence in leaf respiration from estimates of thermal acclimation across time and space. *New Phytologist*, *207*, 1026–1037. https://doi.org/10.1111/nph.13417

Walker, A. P., Beckerman, A. P., Gu, L., Kattge, J., Cernusak, L. A., Domingues, T. F., Scales, J. C., Wohlfahrt, G., Wullschleger, S. D., & Woodward, F. I. (2014). The relationship of leaf photosynthetic traits – Vc_{max} and J_{max} – to leaf nitrogen, leaf phosphorus, and specific leaf area: A meta-analysis and modeling study. *Ecology and Evolution*, *4*, 3218–3235.

Wang, H., Atkin, O. K., Keenan, T. F., Smith, N. G., Wright, I. J., Bloomfield, K. J., Kattge, J., Reich, P. B., & Prentice, I. C. (2020). Acclimation of leaf respiration consistent with optimal photosynthetic capacity. *Global Change Biology*, *26*(4), 2573–2583. https://doi.org/10.1111/gcb.14980

Ward, N. D., Megonigal, J. P., Bond-Lamberty, B., Bailey, V. L., Butman, D., Canuel, E. A., Diefenderfer, H., Ganju, N. K., Goñi, M. A., Graham, E. B., Hopkinson, C. S., Khangaonkar, T., Langley, J. A., McDowell, N. G., Myers-Pigg, A. N., Neumann, R. B., Osburn, C. L., Price, R. M., Rowland, J., … Windham-Myers, L. (2020). Representing the function and sensitivity of coastal interfaces in earth system models. *Nature Communications*, *11*(1), 2458. https://doi.org/10.1038/s41467-020-16236-2

Way, D. A., & Sage, R. F. (2008). Thermal acclimation of photosynthesis in black spruce (*Picea mariana* (Mill.) B.S.P.). *Plant, Cell and Environment*, *31*, 1250–1262.

Way, D. A., & Yamori, W. (2014). Thermal acclimation of photosynthesis: On the importance of adjusting our definitions and accounting for thermal acclimation of respiration. *Photosynthesis Research*, *119*, 89–100. https://doi.org/10.1007/s11120-013-9873-7

Weaver, C. A., & Armitage, A. R. (2020). Above- and belowground responses to nutrient enrichment within a marsh-mangrove ecotone. *Estuarine, Coastal and Shelf Science*, *243*, 106884.

Wright, I. J., Reich, P. B., Westoby, M., Ackerly, D. D., Baruch, Z., Bongers, F., Cavender-Bares, J., Chapin, T., Cornelissen, J. H. C., Diemer, M., Flexas, J., Garnier, E., Groom, P. K., Gulias, J., Hikosaka, K., Lamont, B. B., Lee, T., Lee, W., Lusk, C., … Villar, R. (2004). The worldwide leaf economics spectrum. *Nature*, *428*, 821–827. https://doi.org/10.1038/nature02403

Yamori, W., Hikosaka, K., & Way, D. A. (2014). Temperature response of photosynthesis in C_3, C_4, and CAM plants: Temperature acclimation and temperature adaptation. *Photosynthesis Research*, *119*, 101–117. https://doi.org/10.1007/s11120-013-9874-6

Zaragoza-Castells, J., Sanchez-Gomez, D., Valladares, F., Hurry, V., & Atkin, O. K. (2007). Does growth irradiance affect temperature dependence and thermal acclimation of leaf respiration? Insights from a Mediterranean tree with long-lived leaves. *Plant, Cell and Environment*, *30*, 820–833. https://doi.org/10.1111/j.1365-3040.2007.01672.x

SUPPORTING INFORMATION

Additional supporting information may be found in the online version of the article at the publisher's website.

How to cite this article: Sturchio, M. A., Chieppa, J., Chapman, S. K., Canas, G., & Aspinwall, M. J. (2021). Temperature acclimation of leaf respiration differs between marsh and mangrove vegetation in a coastal wetland ecotone. *Global Change Biology*, 00, 1–18. https://doi.org/10.1111/gcb.15938